

Explicit form of the “modified point mass trajectory model” for the use in Fire Control Systems

 L. BARANOWSKI^{1*}, P. MAJEWSKI², and J. SZYMONIK²
¹Military University of Technology, Faculty of Mechatronics and Aerospace, ul. gen. Sylwestra Kaliskiego 2, 00-908 Warsaw, Poland

²PIT-RADWAR S.A., Bureau for Air-Defence Systems, ul. Poligonowa 30, 04-051 Warsaw, Poland

Abstract. The main objective of this article is to obtain equations of motion of the spin-stabilized projectile in the presence of non-constant wind. Introducing models allowing utilization of inhomogeneous wind is dictated by new possibilities created by the use of e.g. lidars in the Fire Control Systems (FCS). Constant feed of wind data can replace meteorological messages, increasing the FCS effectiveness. Article contains results of projectile flight simulations which indicate the positive effect that the derived explicit form of the model has when considering software development for modern Fire Control Systems.

Key words: ballistics, equations of motion, projectile path, modified point mass trajectory model, MPMTM, projectile deflection.

1. Introduction

In the literature, various models of a projectile’s motion are discussed:

- the point mass trajectory model [1, 2];
- the rigid body trajectory model [1, 3–5];
- the modified point mass trajectory model [2, 6–9].

This paper is focused on the last one – moderately complex and able to describe the motion of the projectile sufficiently. This model has four degrees of freedom (three coordinates of the center of mass and angular rate around the axis of symmetry) – one degree more than the simplest point mass motion model. It was pointed out that this model was originally written in the implicit form. The comparison of the results and simulation time of the projectile’s flight calculated using the modified point mass trajectory model in its implicit form and rigid body motion model can be found in [7] and [10]. The system of equations is as follows

$$\dot{\mathbf{x}} = \mathbf{u}, \quad (1a)$$

$$m \cdot \dot{\mathbf{u}} = \mathbf{DF} + \mathbf{LF} + \mathbf{MF} + m\mathbf{g} + m\mathbf{\Lambda} = \mathbf{AF} + \mathbf{EF}, \quad (1b)$$

$$I_x \cdot \dot{p} = \mathbf{SDM}, \quad (1c)$$

where $\mathbf{x} = [x, y, z]$ (Fig. 1) is the three-dimensional position vector, \mathbf{u} is the velocity vector with respect to a ground reference system, p is the angular velocity of the spinning motion, \mathbf{SDM} is the torque slowing down the spin

*e-mail: leszek.baranowski@wat.edu.pl

Manuscript submitted 2019-09-24, revised 2020-03-30, initially accepted for publication 2020-05-28, published in October 2020

$$\mathbf{SDM} = \frac{\rho v^2}{2} S d C_{\text{spin}} \frac{pd}{v}, \quad (2)$$

and \mathbf{DF} , \mathbf{LF} , \mathbf{MF} , $m\mathbf{g}$, $m\mathbf{\Lambda}$ are the drag force, lift force, Magnus force, gravitational force, Coriolis force respectively.

$$\mathbf{DF} = -\frac{\rho v^2}{2} S (C_{D0} + C_{D\alpha^2} \cdot \alpha_e^2) \frac{\mathbf{v}}{v}, \quad (3a)$$

$$\mathbf{LF} = \mathbf{LF} = \frac{\rho v^2}{2} S (C_{L\alpha} + C_{L\alpha^3} \cdot \alpha_e^2) \boldsymbol{\alpha}_e, \quad (3b)$$

$$\mathbf{MF} = -\frac{\rho v^2}{2} S \frac{pd}{v} C_{\text{mag-f}} \boldsymbol{\alpha}_e \times \frac{\mathbf{v}}{v}. \quad (3c)$$

\mathbf{AF} denotes the sum of all the partial aerodynamic forces (\mathbf{DF} , \mathbf{LF} , \mathbf{MF}) and \mathbf{EF} – total external forces ($m\mathbf{g}$, $m\mathbf{\Lambda}$). Coefficients of aerodynamic forces used in Eqs. (3):

- C_{D0} drag force coefficient,
- $C_{D\alpha^2}$ induced drag force coefficient,
- $C_{L\alpha}$ lift force coefficient,
- $C_{L\alpha^3}$ cubic lift force coefficient,
- $C_{\text{mag-f}}$ Magnus force coefficient,
- C_{spin} spin damping coefficient.

The trouble with this model lies within the expression for the yaw of repose vector $\boldsymbol{\alpha}_e$. In order to calculate the $\boldsymbol{\alpha}_e$ it has to satisfy the equality condition between the overturning aerodynamic moment of force and the stabilizing torque of the gyroscopic precession [2, 7]:

$$\frac{\rho v^2}{2} S d (C_{M\alpha} + C_{M\alpha^3} \cdot \alpha_e^2) \boldsymbol{\alpha}_e = -I_x p \frac{\mathbf{v} \times \dot{\mathbf{u}}}{v^2}. \quad (4)$$

In the above equation: $C_{M\alpha}$ is the overturning moment coefficient and $C_{M\alpha^3}$ is the cubic overturning moment coefficient. It is

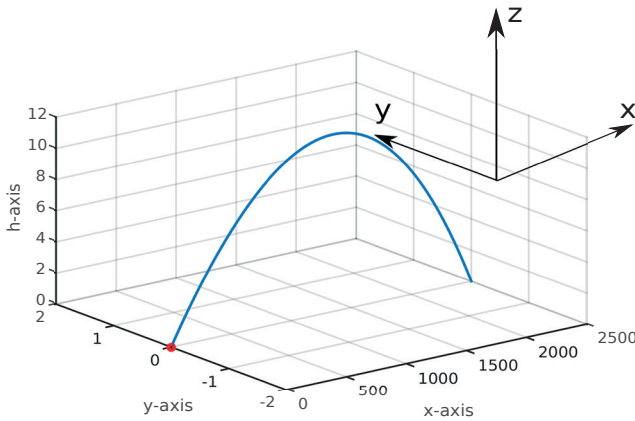


Fig. 1. Coordination system used in calculations

easily seen that vector α_e depends on $\dot{\mathbf{u}}$, which makes the differential equation being defined by an implicit function. Therefore, the main objective of the study [11] was to present a way to obtain an explicit form of the modified point mass model. The explicit form of the mathematical motion model was derived under some additional assumptions:

- in the equations for the aerodynamic forces only the terms up to $\mathcal{O}(\alpha_e^2)$ order are being considered;
- the wind velocity derivative is set to zero

$$\dot{\mathbf{w}} \equiv 0, \quad (5)$$

which means that the wind is constant along the projectile's flight path.

Furthermore, the Cartesian coordinate system for the velocity vector \mathbf{v} was changed into spherical coordinate system, which was the key factor to develop the explicit form of the modified point mass model. The final form of the explicit system of ODEs (equivalent to the modified point mass model) is as follows (Eqs. (62a)–(62d) in [11])

$$\dot{\mathbf{x}} = \mathbf{v} + \mathbf{w}, \quad (6)$$

where \mathbf{x} is the three-dimensional position vector,

$$\dot{p} = \frac{\rho v^2}{2I_x} S d C_{spin} \cdot \hat{p}, \quad S = \frac{\pi d^2}{4}, \quad (7)$$

$$\dot{v} = -\frac{\rho v^2}{2m} S \left(C_{D0} + \hat{C}_{D\alpha^2} \left(\frac{2mg}{\rho v^2 S} \right)^2 \right. \\ \left. \frac{\hat{I}_x^2 \hat{p}^2 \cos^2(\gamma_a)}{\left(1 - \hat{I}_x \hat{p}^2 \hat{C}_{mag-f} \right)^2 + \left(\hat{I}_x \hat{p} \hat{C}_{L\alpha} \right)^2} \right) - g \sin(\gamma_a), \quad (8)$$

$$\begin{bmatrix} \dot{\gamma}_a \\ \dot{\chi}_a \cos(\gamma_a) \end{bmatrix} = -\frac{g}{v} \frac{\cos(\gamma_a)}{\left(1 - \hat{I}_x \hat{p}^2 \hat{C}_{mag-f} \right)^2 + \left(\hat{I}_x \hat{p} \hat{C}_{L\alpha} \right)^2} \\ \begin{bmatrix} 1 - \hat{I}_x \hat{p}^2 \hat{C}_{mag-f} \\ \hat{I}_x \hat{p} \hat{C}_{L\alpha} \end{bmatrix}, \quad (9)$$

$$\hat{I}_x = \frac{I_x}{m d^2}, \quad \hat{p} = \frac{p d}{v},$$

$$\hat{C}_{D\alpha^2} = \frac{C_{D\alpha^2}}{C_{M\alpha}^2}, \quad \hat{C}_{L\alpha} = \frac{C_{L\alpha}}{C_{M\alpha}}, \quad \hat{C}_{mag-f} = \frac{C_{mag-f}}{C_{M\alpha}},$$

I_x axial moment of inertia,

γ_a elevation of the velocity vector in the global reference frame,

χ_a azimuth of the velocity vector in the global reference frame.

The derivation of the model presented in [11] was conducted for homogeneous wind (5). This paper focuses on the model's equation derivation for the non-constant wind.

The derived explicit trajectory model can be used in Fire Control Systems. Its improved form (with comparison to the implicit form) is suitable for fast algorithms [12] for projectile impact point calculation, as well as for projectile aerodynamic characteristics identification [13].

In 1990 J.W. Bradley [14] made an attempt to derive explicit form of the modified point mass trajectory model presented in [6]. However, the report lacks depth in both describing the problem as well as in solving it. It is important to notice differences between this paper and the report by J.W. Bradley:

1. Bradley derived the model based on the implicit form of the Lieske model presented in [6], where the coefficients of the lift force and the overturning moment are linearly dependent on the yaw of repose. Bradley, in order to derive the explicit form of the model, omitted the Magnus force coefficient in the formula for yaw of repose.
2. The model presented in this paper was derived based on the implicit form of the modified point mass trajectory model presented in [2], where coefficients for the lift force and the overturning moment depend non-linearly on the yaw of repose.
3. Bradley derived vector equations. Authors present also the scalar form of the model in the reference system associated with projectile's velocity.
4. Bradley did not take into account the influence of the inhomogeneous wind, which is the main subject of this article.

2. Broader view: including non-homogeneous wind, discussing generalizations

2.1. Preliminaries: general wind. Through current study, the wind will be considered variable other than what was previously considered [11] (i.e. $\dot{\mathbf{w}} \equiv 0$). Now this assumption will be dropped, and it will be shown that morally nothing changes with the M-model. In some sense, all the effects of the wind will be incorporated into the external forces **EF**. At the beginning let us stress that one needs to be careful and must not mix \mathbf{v} and \mathbf{u} , the former is the velocity of the air-flow, whereas the latter – the velocity of the projectile with respect to a ground reference system. It holds that

$$\mathbf{v} = \mathbf{u} - \mathbf{w}, \quad (10)$$

which obviously implies

$$\dot{\mathbf{u}} = \dot{\mathbf{v}} + \dot{\mathbf{w}}. \quad (11)$$

Recall that in general terms the implicit differential system was

$$\dot{\mathbf{x}} = \mathbf{u}, \quad (12)$$

$$m\dot{\mathbf{u}} = \mathbf{AF} + \mathbf{EF}^{(0)}, \quad (13)$$

$$I_x \dot{p} = \text{SDM}. \quad (14)$$

The external forces have been ornamented by a superscript which tells that those are the original external forces – in a moment wind corrections to external forces will be derived. Moreover, authors decided to use the direction of \mathbf{v} to define the airframe reference system. Thus, the second equation needs to be modified:

$$\dot{\mathbf{x}} = \mathbf{v} + \mathbf{w}, \quad (15)$$

$$m\dot{\mathbf{v}} = \mathbf{AF} + \mathbf{EF}^{(0)} - m\dot{\mathbf{w}}, \quad (16)$$

$$I_x \dot{p} = \text{SDM}. \quad (17)$$

The derivation in [11] (specifically Eq. (26) in [11]) assumed that $\boldsymbol{\alpha}_e$ was proportional to $\hat{\mathbf{e}}_v \times \dot{\mathbf{v}}$, where

$$\hat{\mathbf{e}}_v = \begin{bmatrix} \cos \gamma_a \cos \chi_a \\ \cos \gamma_a \sin \chi_a \\ \sin \gamma_a \end{bmatrix}. \quad (18)$$

This was due to the fact that $\dot{\mathbf{v}}$ was the same as $\dot{\mathbf{u}}$ which is no longer true. The task is to calculate $\hat{\mathbf{e}}_v \times \dot{\mathbf{u}}$ because (recall (4))

$$C_{M\alpha} \cdot \boldsymbol{\alpha}_e = -\frac{2m}{\rho v^2 S} \hat{I}_x \hat{p} \hat{\mathbf{e}}_v \times \dot{\mathbf{u}}. \quad (19)$$

However, to cope with this let us first discuss the general wind. The general wind is a function $\mathbf{w}(\mathbf{x}, t)$. Therefore

$$\begin{aligned} \dot{\mathbf{w}} &= (\nabla_{\mathbf{x}} \mathbf{w}) \cdot \dot{\mathbf{x}} + \frac{\partial \mathbf{w}}{\partial t} \\ &= (\nabla_{\mathbf{x}} \mathbf{w}) \cdot \mathbf{u} + \frac{\partial \mathbf{w}}{\partial t} \\ &= (\nabla_{\mathbf{x}} \mathbf{w}) \cdot (\mathbf{v} + \mathbf{w}) + \frac{\partial \mathbf{w}}{\partial t}. \end{aligned} \quad (20)$$

By using (11) one gets that

$$\hat{\mathbf{e}}_v \times \dot{\mathbf{u}} = \hat{\mathbf{e}}_v \times \dot{\mathbf{v}} + \hat{\mathbf{e}}_v \times \dot{\mathbf{w}} \quad (21)$$

and when confronted with (20) one notices that the second summand does not depend on $\dot{\mathbf{u}}$ nor $\dot{\mathbf{v}}$! Thanks to this the previous derivation still holds, there is only a need for some redefinitions.

First, using (20)

$$\begin{aligned} C_{M\alpha} \cdot \boldsymbol{\alpha}_e &= -\frac{2m}{\rho v^2 S} \hat{I}_x \hat{p} \hat{\mathbf{e}}_v \times \dot{\mathbf{u}} \\ &= -\frac{2m}{\rho v^2 S} \hat{I}_x \hat{p} (\hat{\mathbf{e}}_v \times \dot{\mathbf{v}} + \hat{\mathbf{e}}_v \times \dot{\mathbf{w}}) \\ &= C_{M\alpha} \cdot (\boldsymbol{\alpha}_e^{(0)} + \boldsymbol{\alpha}_e^{(\dot{\mathbf{w}})}). \end{aligned} \quad (22)$$

Both \mathbf{LF} and \mathbf{MF} are linear with respect to $\boldsymbol{\alpha}_e$ thus the wind-term can be shifted toward the external forces \mathbf{EF} .

2.2. Modified external forces. In (22) it was argued that the vector $\boldsymbol{\alpha}_e$ in the case of general wind is the sum of the homogeneous part and the $\dot{\mathbf{w}}$ -part, which was zero in case of the homogeneous wind. Now the aerodynamic forces take the form

$$\begin{aligned} \mathbf{LF} &= -m \hat{C}_{L\alpha} \hat{I}_x \hat{p} (\hat{\mathbf{e}}_v \times \dot{\mathbf{v}} + \hat{\mathbf{e}}_v \times \dot{\mathbf{w}}) \\ &= \mathbf{LF}^{(0)} + \mathbf{LF}^{(\dot{\mathbf{w}})}, \end{aligned} \quad (23)$$

$$\begin{aligned} \mathbf{MF} &= -m \hat{C}_{\text{mag-f}} \hat{I}_x \hat{p}^2 \hat{\mathbf{e}}_v \times (\hat{\mathbf{e}}_v \times \dot{\mathbf{v}} + \hat{\mathbf{e}}_v \times \dot{\mathbf{w}}) \\ &= \mathbf{MF}^{(0)} + \mathbf{MF}^{(\dot{\mathbf{w}})}. \end{aligned} \quad (24)$$

the paper introduced the convention that \mathbf{AF} are aerodynamic forces dependent on $\boldsymbol{\alpha}_e$, this notion needs to be more precise, namely \mathbf{AF} will stand for all the forces that depend implicitly on $\dot{\mathbf{u}}$, i.e. on $\boldsymbol{\alpha}_e^{(0)}$. Therefore

$$\mathbf{AF}(\mathbf{x}, \mathbf{u}, p; \mathbf{w}, \boldsymbol{\alpha}_e^{(0)}) = \mathbf{DF} + \mathbf{LF}^{(0)} + \mathbf{MF}^{(0)} \quad (25)$$

and

$$\begin{aligned} \mathbf{EF}(\mathbf{x}, \mathbf{u}, p; \mathbf{w}) &= \mathbf{EF}^{(0)} + \mathbf{LF}^{(\dot{\mathbf{w}})} + \mathbf{MF}^{(\dot{\mathbf{w}})} - m\dot{\mathbf{w}} \\ &= \mathbf{EF}^{(0)} + \mathbf{EF}^{(\dot{\mathbf{w}})}. \end{aligned} \quad (26)$$

Above, in (26) the symbol $\mathbf{EF}^{(0)}$ stands for the initial forces excluding the interaction with the wind, e.g. the gravitational force, the Coriolis force, the global corrections etc. As before the explicit form of $\mathbf{EF}^{(0)}$ is irrelevant to the derivation. The $\dot{\mathbf{w}}$ -part of the external forces is

$$\begin{aligned} \mathbf{EF}^{(\dot{\mathbf{w}})} &= -m \hat{I}_x \hat{p} \left(\hat{C}_{L\alpha} \hat{\mathbf{e}}_v \times \dot{\mathbf{w}} + \right. \\ &\quad \left. + \hat{p} \hat{C}_{\text{mag-f}} \hat{\mathbf{e}}_v \times (\hat{\mathbf{e}}_v \times \dot{\mathbf{w}}) \right) - m\dot{\mathbf{w}} \\ &= -m \hat{I}_x \hat{p} \left(\hat{C}_{L\alpha} \hat{\mathbf{e}}_v \times \dot{\mathbf{w}} + \right. \\ &\quad \left. - \hat{p} \hat{C}_{\text{mag-f}} (\dot{\mathbf{w}} - (\hat{\mathbf{e}}_v \circ \dot{\mathbf{w}}) \cdot \hat{\mathbf{e}}_v) \right) - m\dot{\mathbf{w}} \\ &= -m \hat{I}_x \hat{p} \cdot \hat{\mathbf{e}}_v \times \left(\hat{C}_{L\alpha} \dot{\mathbf{w}} + \right. \\ &\quad \left. + \hat{p} \hat{C}_{\text{mag-f}} \hat{\mathbf{e}}_v \times \dot{\mathbf{w}} \right) - m\dot{\mathbf{w}}. \end{aligned} \quad (27)$$

From the form (27) of the wind correction $\mathbf{EF}^{(\dot{\mathbf{w}})}$ one notices at first that

$$\mathbf{EF}^{(\dot{\mathbf{w}})} \circ \hat{\mathbf{e}}_v = -m \dot{\mathbf{w}} \circ \hat{\mathbf{e}}_v. \quad (28)$$

Moreover, by elementary algebra

$$\mathbf{EF}^{(\dot{\mathbf{w}})} \circ \hat{\mathbf{e}}_{\boldsymbol{\gamma}} = m \hat{I}_x \hat{\rho} \left(\hat{\rho} \hat{\mathbf{C}}_{\text{mag-f}} \dot{\mathbf{w}} \circ \hat{\mathbf{e}}_{\boldsymbol{\gamma}} + \right. \\ \left. - \hat{\mathbf{C}}_{L\alpha} \dot{\mathbf{w}} \circ \hat{\mathbf{e}}_{\boldsymbol{\chi}} \right) - m \dot{\mathbf{w}} \circ \hat{\mathbf{e}}_{\boldsymbol{\gamma}}, \quad (29)$$

$$\mathbf{EF}^{(\dot{\mathbf{w}})} \circ \hat{\mathbf{e}}_{\boldsymbol{\chi}} = m \hat{I}_x \hat{\rho} \left(\hat{\mathbf{C}}_{L\alpha} \dot{\mathbf{w}} \circ \hat{\mathbf{e}}_{\boldsymbol{\gamma}} + \right. \\ \left. + \hat{\rho} \hat{\mathbf{C}}_{\text{mag-f}} \dot{\mathbf{w}} \circ \hat{\mathbf{e}}_{\boldsymbol{\chi}} \right) - m \dot{\mathbf{w}} \circ \hat{\mathbf{e}}_{\boldsymbol{\chi}}. \quad (30)$$

By using the same matrices \mathbf{M} and \mathbf{K} as defined in [11] (Eqs. (33) and (35) in [11]):

$$\mathbf{M} = \begin{bmatrix} \hat{\rho} \hat{\mathbf{C}}_{\text{mag-f}} & -\hat{\mathbf{C}}_{L\alpha} \\ \hat{\mathbf{C}}_{L\alpha} & \hat{\rho} \hat{\mathbf{C}}_{\text{mag-f}} \end{bmatrix}, \quad (31)$$

$$\mathbf{K} = 1 - \hat{I}_x \hat{\rho} \mathbf{M} \\ = \begin{bmatrix} 1 - \hat{I}_x \hat{\rho}^2 \hat{\mathbf{C}}_{\text{mag-f}} & \hat{I}_x \hat{\rho} \hat{\mathbf{C}}_{L\alpha} \\ -\hat{I}_x \hat{\rho} \hat{\mathbf{C}}_{L\alpha} & 1 - \hat{I}_x \hat{\rho}^2 \hat{\mathbf{C}}_{\text{mag-f}} \end{bmatrix}, \quad (32)$$

it stands that

$$\begin{bmatrix} \mathbf{EF}^{(\dot{\mathbf{w}})} \circ \hat{\mathbf{e}}_{\boldsymbol{\gamma}} \\ \mathbf{EF}^{(\dot{\mathbf{w}})} \circ \hat{\mathbf{e}}_{\boldsymbol{\chi}} \end{bmatrix} = -m \left(1 - \hat{I}_x \hat{\rho} \mathbf{M} \right) \begin{bmatrix} \dot{\mathbf{w}} \circ \hat{\mathbf{e}}_{\boldsymbol{\gamma}} \\ \dot{\mathbf{w}} \circ \hat{\mathbf{e}}_{\boldsymbol{\chi}} \end{bmatrix} \\ = -m \mathbf{K} \begin{bmatrix} \dot{\mathbf{w}} \circ \hat{\mathbf{e}}_{\boldsymbol{\gamma}} \\ \dot{\mathbf{w}} \circ \hat{\mathbf{e}}_{\boldsymbol{\chi}} \end{bmatrix}. \quad (33)$$

Recall the equation

$$\begin{bmatrix} \dot{\gamma}_a \\ \dot{\chi}_a \cos \gamma_a \end{bmatrix} = \frac{1}{m v} \frac{1}{\det \mathbf{K}} \mathbf{K}^T \cdot \begin{bmatrix} \mathbf{EF} \circ \hat{\mathbf{e}}_{\boldsymbol{\gamma}} \\ \mathbf{EF} \circ \hat{\mathbf{e}}_{\boldsymbol{\chi}} \end{bmatrix}, \quad (34)$$

which was derived in [11] (Eq. (39)). If the wind correction (26) is applied, then:

$$\begin{bmatrix} \dot{\gamma}_a \\ \dot{\chi}_a \cos \gamma_a \end{bmatrix} = \frac{1}{m v} \frac{1}{\det \mathbf{K}} \mathbf{K}^T \\ \left(\begin{bmatrix} \mathbf{EF}^{(0)} \circ \hat{\mathbf{e}}_{\boldsymbol{\gamma}} \\ \mathbf{EF}^{(0)} \circ \hat{\mathbf{e}}_{\boldsymbol{\chi}} \end{bmatrix} + \begin{bmatrix} \mathbf{EF}^{(\dot{\mathbf{w}})} \circ \hat{\mathbf{e}}_{\boldsymbol{\gamma}} \\ \mathbf{EF}^{(\dot{\mathbf{w}})} \circ \hat{\mathbf{e}}_{\boldsymbol{\chi}} \end{bmatrix} \right). \quad (35)$$

Using (33) and the fact that $\mathbf{K} \cdot \mathbf{K}^T = \det \mathbf{K} \cdot 1$, Eq. (35) becomes

$$\begin{bmatrix} \dot{\gamma}_a \\ \dot{\chi}_a \cos \gamma_a \end{bmatrix} = \frac{1}{m v} \frac{1}{\det \mathbf{K}} \mathbf{K}^T \cdot \begin{bmatrix} \mathbf{EF}^{(0)} \circ \hat{\mathbf{e}}_{\boldsymbol{\gamma}} \\ \mathbf{EF}^{(0)} \circ \hat{\mathbf{e}}_{\boldsymbol{\chi}} \end{bmatrix} + \\ - \frac{1}{v} \begin{bmatrix} \dot{\mathbf{w}} \circ \hat{\mathbf{e}}_{\boldsymbol{\gamma}} \\ \dot{\mathbf{w}} \circ \hat{\mathbf{e}}_{\boldsymbol{\chi}} \end{bmatrix}. \quad (36)$$

Then, $\boldsymbol{\alpha}_e^2$ can be obtained based on Eqs. (22) and (47) in [11]

$$\| \mathbf{C}_{M\alpha} \cdot \boldsymbol{\alpha}_e \|^2 = \left\| \mathbf{C}_{M\alpha} \cdot \left(\boldsymbol{\alpha}_e^{(0)} + \boldsymbol{\alpha}_e^{(\dot{\mathbf{w}})} \right) \right\|^2 \\ = \left(\frac{2 \hat{I}_x \hat{\rho}}{\rho v^2 S} \right)^2 \frac{1}{\det \mathbf{K}} \\ \left(\left(\mathbf{EF}^{(0)} \circ \hat{\mathbf{e}}_{\boldsymbol{\gamma}} \right)^2 + \left(\mathbf{EF}^{(0)} \circ \hat{\mathbf{e}}_{\boldsymbol{\chi}} \right)^2 \right). \quad (37)$$

The effect of the inhomogeneous wind on the motion of the projectile has been discussed and analyzed carefully. Now it is time to sum-up results and present the M-model including general wind. Maybe one does not notice yet, after this cumbersome proof, but the wind effect shows itself as very simple.

2.3. Final form of the M-model with general wind. The derivation of the explicit M-model has been refined to include a general wind. The form is almost the same as in [11] (Eqs. (49a)–(49d) in [11]) where the results in case of $\dot{\mathbf{w}} \equiv 0$ have been presented. The key observation here is that including the general wind into the model requires us only to modify the external forces \mathbf{EF} . Below, $\mathbf{EF}^{(0)}$ should be treated as the original external forces one wanted to have acting on the projectile—excluding the wind corrections.

The differential equations for the M-model with general wind are as follow:

$$\dot{\mathbf{x}} = \mathbf{v} + \mathbf{w}, \quad (38)$$

$$\dot{\rho} = \frac{\rho v^2}{2 I_x} S d C_{\text{spin}} \cdot \hat{\rho}, \quad (39)$$

$$\dot{v} = -\frac{\rho v^2}{2m} S \left(C_{D0} + \hat{\mathbf{C}}_{D\alpha^2} \left(\frac{2 \hat{I}_x \hat{\rho}}{\rho v^2 S} \right)^2 \right. \\ \left. \frac{\left(\mathbf{EF}^{(0)} \circ \hat{\mathbf{e}}_{\boldsymbol{\gamma}} \right)^2 + \left(\mathbf{EF}^{(0)} \circ \hat{\mathbf{e}}_{\boldsymbol{\chi}} \right)^2}{\det \mathbf{K}} \right) + \\ + \frac{1}{m} \mathbf{EF}^{(0)} \circ \hat{\mathbf{e}}_{\mathbf{v}} - \dot{\mathbf{w}} \circ \hat{\mathbf{e}}_{\mathbf{v}}, \quad (40)$$

and

$$\begin{bmatrix} \dot{\gamma}_a \\ \dot{\chi}_a \cos \gamma_a \end{bmatrix} = \frac{1}{m v} \frac{1}{\det \mathbf{K}} \mathbf{K}^T \cdot \\ \begin{bmatrix} \mathbf{EF}^{(0)} \circ \hat{\mathbf{e}}_{\boldsymbol{\gamma}} \\ \mathbf{EF}^{(0)} \circ \hat{\mathbf{e}}_{\boldsymbol{\chi}} \end{bmatrix} - \frac{1}{v} \begin{bmatrix} \dot{\mathbf{w}} \circ \hat{\mathbf{e}}_{\boldsymbol{\gamma}} \\ \dot{\mathbf{w}} \circ \hat{\mathbf{e}}_{\boldsymbol{\chi}} \end{bmatrix}. \quad (41)$$

To define the system (38)–(41) the same definitions as in [11] were used. That is

$$\mathbf{K}^T = \begin{bmatrix} 1 - \hat{I}_x \hat{\rho}^2 \hat{\mathbf{C}}_{\text{mag-f}} & -\hat{I}_x \hat{\rho} \hat{\mathbf{C}}_{L\alpha} \\ \hat{I}_x \hat{\rho} \hat{\mathbf{C}}_{L\alpha} & 1 - \hat{I}_x \hat{\rho}^2 \hat{\mathbf{C}}_{\text{mag-f}} \end{bmatrix} \quad (42)$$

and

$$\det \mathbf{K} = \left(1 - \hat{I}_x \hat{p}^2 \hat{C}_{\text{mag-f}}\right)^2 + \left(\hat{I}_x \hat{p} \hat{C}_{L\alpha}\right)^2. \quad (43)$$

Moreover

$$\hat{I}_x = \frac{I_x}{m d^2}, \quad \hat{p} = \frac{p d}{v}. \quad (44)$$

The dimensionless “hatted” coefficients are again given as

$$\begin{aligned} \hat{C}_{D\alpha^2} &= \frac{C_{D\alpha^2}}{C_{M\alpha}^2}, & \hat{C}_{L\alpha} &= \frac{C_{L\alpha}}{C_{M\alpha}}, \\ \hat{C}_{\text{mag-f}} &= \frac{C_{\text{mag-f}}}{C_{M\alpha}}. \end{aligned} \quad (45)$$

Also recall that \mathbf{v} is the velocity of the air-flow and $\mathbf{v} = \mathbf{u} - \mathbf{w}$. Thus one should not forget to subtract the wind from the initial velocity of the projectile.

Let us only recall the meaning of $\boldsymbol{\alpha}_e^{(0)}$ and $\boldsymbol{\alpha}_e^{(\dot{w})}$. Again, it holds that

$$\begin{aligned} C_{M\alpha} \cdot \boldsymbol{\alpha}_e &= C_{M\alpha} \cdot \left(\boldsymbol{\alpha}_e^{(0)} + \boldsymbol{\alpha}_e^{(\dot{w})}\right) \\ &= \frac{2\hat{I}_x \hat{p}}{\rho v^2 S} \frac{1}{\det \mathbf{K}} \begin{bmatrix} \hat{\mathbf{e}}_x & -\hat{\mathbf{e}}_y \end{bmatrix} \mathbf{K}^T \begin{bmatrix} \mathbf{EF}^{(0)} \circ \hat{\mathbf{e}}_y \\ \mathbf{EF}^{(0)} \circ \hat{\mathbf{e}}_x \end{bmatrix} \end{aligned} \quad (46)$$

and

$$\begin{aligned} \|\mathbf{C}_{M\alpha} \cdot \boldsymbol{\alpha}_e\|^2 &= \left(\frac{2\hat{I}_x \hat{p}}{\rho v^2 S}\right)^2 \\ &\quad \frac{\left(\mathbf{EF}^{(0)} \circ \hat{\mathbf{e}}_y\right)^2 + \left(\mathbf{EF}^{(0)} \circ \hat{\mathbf{e}}_x\right)^2}{\det \mathbf{K}}. \end{aligned} \quad (47)$$

It is worth to recall then, that

$$C_{M\alpha} \cdot \boldsymbol{\alpha}_e^{(\dot{w})} = \frac{2m\hat{I}_x \hat{p}}{\rho v^2 S} \dot{\mathbf{w}} \times \hat{\mathbf{e}}_v. \quad (48)$$

The system (38)–(41) is an extension to the one presented in [11] including general wind. However, the physical effects of this details might not even be important but nevertheless for the sake of the completeness of the presentation authors feel the need to elaborate on this matter.

2.4. Example of an M-model: projectile motion influenced by constant gravitational force with altitude-dependent wind. In this section an example for an inhomogeneous wind is presented. To simplify, as one should do when showing examples, altitude-dependent cross-wind will be considered, i.e. y-wind. Assumption:

$$\mathbf{w}(\mathbf{x}, t) = \begin{bmatrix} 0 \\ w_y(z, t) \\ 0 \end{bmatrix} = w_y(z, t) \cdot \hat{\mathbf{e}}_y. \quad (49)$$

Exactly in the same way as in the [11] it will be considered that the average gravitational acceleration to be the only source of

acceleration. Thus

$$\mathbf{EF}^{(0)} = -mg \hat{\mathbf{e}}_z = -mg (\sin \gamma_a \hat{\mathbf{e}}_v + \cos \gamma_a \hat{\mathbf{e}}_y). \quad (50)$$

2.4.1. The system of differential equations. Finally, after illustrating all assumptions used in this example system of equations can be written in full extent. First, the explicit expression for $\dot{\mathbf{w}}$ will be presented. Recall, that (Eq. (20))

$$\dot{\mathbf{w}} = (\nabla_{\mathbf{x}} \mathbf{w}) \cdot (\mathbf{v} + \mathbf{w}) + \frac{\partial \mathbf{w}}{\partial t}. \quad (51)$$

It is true that in the example under consideration

$$\nabla_{\mathbf{x}} \mathbf{w} = \frac{\partial w_y}{\partial z} \cdot \hat{\mathbf{e}}_y \otimes \hat{\mathbf{e}}_z^T = \frac{\partial w_y}{\partial z} \cdot \begin{bmatrix} 0 & 0 & 0 \\ 0 & 0 & 1 \\ 0 & 0 & 0 \end{bmatrix}. \quad (52)$$

Then

$$\dot{\mathbf{w}} = \frac{\partial w_y}{\partial z} \cdot (\mathbf{v} \circ \hat{\mathbf{e}}_z + \mathbf{w} \circ \hat{\mathbf{e}}_z) \cdot \hat{\mathbf{e}}_y + \frac{\partial \mathbf{w}}{\partial t}, \quad (53)$$

which then simplifies to the final

$$\dot{\mathbf{w}} = \left(v \sin \gamma_a \frac{\partial w_y}{\partial z} + \frac{\partial w_y}{\partial t}\right) \cdot \hat{\mathbf{e}}_y. \quad (54)$$

The explicit form of the needed scalar products can be quickly computed. It stands that

$$\dot{\mathbf{w}} \circ \hat{\mathbf{e}}_v = \left(v \sin \gamma_a \frac{\partial w_y}{\partial z} + \frac{\partial w_y}{\partial t}\right) \cdot \cos \gamma_a \sin \chi_a, \quad (55)$$

$$\dot{\mathbf{w}} \circ \hat{\mathbf{e}}_y = \left(v \sin \gamma_a \frac{\partial w_y}{\partial z} + \frac{\partial w_y}{\partial t}\right) \cdot \sin \gamma_a \sin \chi_a, \quad (56)$$

$$\dot{\mathbf{w}} \circ \hat{\mathbf{e}}_x = \left(v \sin \gamma_a \frac{\partial w_y}{\partial z} + \frac{\partial w_y}{\partial t}\right) \cdot \cos \chi_a. \quad (57)$$

The example can be now stated.

An M-model in constant gravitational field with altitude-dependent cross-wind is

$$\dot{\mathbf{x}} = v \cdot \hat{\mathbf{e}}_v + w_y(z, t) \cdot \hat{\mathbf{e}}_y, \quad (58)$$

$$\dot{p} = \frac{\rho v^2}{2I_x} S d C_{\text{spin}} \cdot \hat{p}, \quad (59)$$

$$\begin{aligned} \dot{v} &= -\frac{\rho v^2}{2m} S \left(C_{D0} + \hat{C}_{D\alpha^2} \left(\frac{2mg}{\rho v^2 S} \right)^2 \right. \\ &\quad \left. \frac{\hat{I}_x^2 \hat{p}^2 \cos^2 \gamma_a}{(1 - \hat{I}_x \hat{p}^2 \hat{C}_{\text{mag-f}})^2 + (\hat{I}_x \hat{p} \hat{C}_{L\alpha})^2} \right) + \\ &\quad -g \sin \gamma_a + \\ &\quad - \left(v \sin \gamma_a \frac{\partial w_y}{\partial z} + \frac{\partial w_y}{\partial t} \right) \cdot \cos \gamma_a \sin \chi_a \end{aligned} \quad (60)$$

and

$$v \begin{bmatrix} \dot{\gamma}_a \\ \dot{\chi}_a \cos \gamma_a \end{bmatrix} = - \frac{g \cos \gamma_a}{\left(1 - \hat{I}_x \hat{p}^2 \hat{C}_{mag-f}\right)^2 + \left(\hat{I}_x \hat{p} \hat{C}_{L\alpha}\right)^2} \begin{bmatrix} 1 - \hat{I}_x \hat{p}^2 \hat{C}_{mag-f} \\ \hat{I}_x \hat{p} \hat{C}_{L\alpha} \end{bmatrix} + \left(v \sin \gamma_a \frac{\partial w_y}{\partial z} + \frac{\partial w_y}{\partial t} \right) \begin{bmatrix} \sin \gamma_a \sin \chi_a \\ \cos \chi_a \end{bmatrix}. \quad (61)$$

2.4.2. The initial condition. The initial condition does not require discussion as the ideology is exactly the same as in the example presented in [11] (Eqs. (64)–(68) in [11]). If it is defined that

$$\mathbf{w}_0 = \mathbf{w}(t_0), \quad (62)$$

then the initial conditions are exactly the same as before. Recall

$$v_0 = \|\mathbf{v}_0\| = \|\mathbf{u}_0 - \mathbf{w}_0\|, \quad (63)$$

$$v_0 \sin \gamma_{a0} = \mathbf{v}_0 \circ \hat{\mathbf{e}}_z, \quad (64)$$

$$\tan \chi_{a0} = \frac{\mathbf{v}_0 \circ \hat{\mathbf{e}}_y}{\mathbf{v}_0 \circ \hat{\mathbf{e}}_x}. \quad (65)$$

The initial position \mathbf{x}_0 is arbitrary and p_0 needs to be known a priori or approximated. Thus, the mathematical model of projectile motion for this example is complete.

3. Projectile's parameters and simulation tests results

This section presents projectile's parameters and chosen results of the simulations conducted with the use of both explicit and implicit forms of the modified point mass trajectory model.

3.1. Parameters of the model of training projectile. In the analysis, authors used simulations of firing of a 35 mm anti-aircraft TP-T training projectile (projectile presented in the Fig. 2). The mass-inertia characteristics of the projectile (mass, center of mass and axial moments of inertia) were determined

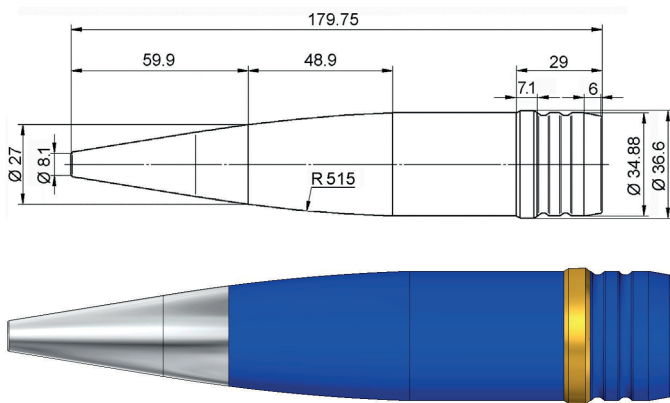


Fig. 2. Basic dimensions and solid model of the 35-mm TP-T projectile

by the theoretical method, using the capabilities of modern design support tools (CAD software). A general view of the projectile with the basic dimensions used to determine the geometric characteristics as well as the model developed in Solid Edge ST3 are shown in Fig. 2. The basic geometric and mass characteristics of the training missile:

- projectile mass $m = 0.55$ kg;
- length of a projectile with a fuse $L = 0.180$ m;
- projectile calibre $d = 0.035$ m;
- projectile axial moment of inertia $I_x = 0.97 \cdot 10^{-4}$ kg m².

The aerodynamic characteristics of the the projectile were calculated using the capabilities of the commercial program PRO-DAS Version 3.5.3 from Arrow Tech, which is a specialized tool for broadly understood computer-aided design of combat means.

The results of calculations of aerodynamic characteristics, assuming the cross-section of the projectile as the characteristic surface $S = \frac{\pi d^2}{4}$ are given in Table 1.

Table 1
Aerodynamic characteristics of a 35 mm TP-T training projectile

Ma	C_{D0}	$C_{D\alpha^2}$	$C_{L\alpha}$	$C_{L\alpha^3}$	C_{mag-f}	C_{spin}	$C_{M\alpha}$
[–]	[–]	[–]	[–]	[–]	[–]	[–]	[–]
0.010	0.182	4.01	1.80	–2.03	–0.380	–0.0128	3.259
0.400	0.186	4.02	1.80	–2.03	–0.380	–0.0130	3.234
0.600	0.187	4.00	1.79	–2.03	–0.380	–0.0129	3.253
0.700	0.187	4.22	1.77	–2.26	–0.385	–0.0128	3.270
0.800	0.196	4.42	1.79	–2.43	–0.395	–0.0126	3.386
0.900	0.232	4.82	1.88	–2.71	–0.425	–0.0124	3.514
0.950	0.290	5.20	1.91	–3.00	–0.545	–0.0121	3.679
0.975	0.331	5.41	1.90	–3.18	–0.485	–0.0121	3.705
1.000	0.374	5.62	1.87	–3.38	–0.445	–0.0122	3.681
1.025	0.398	5.82	1.83	–3.59	–0.425	–0.0120	3.692
1.050	0.414	6.05	1.82	–3.82	–0.410	–0.0116	3.685
1.100	0.407	6.50	1.87	–4.23	–0.380	–0.0108	3.683
1.200	0.389	6.93	1.98	–4.56	–0.345	–0.0098	3.753
1.350	0.365	6.47	2.12	–3.99	–0.310	–0.0090	3.782
1.500	0.347	6.02	2.21	–3.46	–0.295	–0.0085	3.601
2.000	0.287	5.11	2.46	–2.36	–0.265	–0.0076	3.266
2.500	0.239	4.72	2.57	–1.91	–0.260	–0.0066	3.038
3.000	0.204	4.29	2.58	–1.51	–0.260	–0.0061	2.891

The coefficients of aerodynamic drag, lift force and spin dumping moment are interpolated using polynomials in the following form [15, 16]:

$$C(Ma) = (1+s)A(r) + (1-s)B(r), \quad (66)$$

$$A(r) = a_0 + a_1 r + a_2 r^2, \quad (67)$$

$$B(r) = b_0 + b_1 r + b_2 r^2, \quad (68)$$

Explicit form of the “modified point mass trajectory model” for the use in Fire Control Systems

$$r = (Ma^2 - K) / (Ma^2 + K), \quad (69)$$

$$s = \frac{(Ma^2 - K) / (Ma^2 + K)}{\sqrt{(1 - L^2)r^2 + L^2}}, \quad (70)$$

where $C(Ma)$ is an aerodynamic coefficient dependent on the Mach number and $a_0, a_1, a_2, b_0, b_1, b_2, K, L$ are polynomials' parameters. Gridded data piecewise cubic Hermite interpolation (MATLAB griddedInterpolant class) was used to represent induced drag and Magnus force coefficients.

The simulations were carried out in the Earth's system (Fig. 1) with the beginning in the cross-section of the gun barrel. It was assumed that the flight takes place in a standard atmosphere, but taking into account the variable wind and the following initial conditions:

- nominal initial velocity of the projectile – $v_0 = 1180$ m/s,
- nominal rotational speed:

$$p_0 = \frac{2\pi v_0}{27.57d}, \quad (71)$$

where the number 27.57 reflects the length of the revolution of the rifling in caliber units.

3.2. Results. The results of the main numerical studies include:

- the differences in position along the trajectory of the projectile calculated for the maximum range of the projectile – Fig. 4;
- time needed for calculating trajectories for different elevation angles (10 to 710 mil with the step of 20 mil) – in this procedure the fourth order Runge–Kutta method with adaptive step is used – Fig. 5;

The stopping condition for numerical integration was the moment when the projectile reached the point of fall.

The research was carried out in Matlab's environment. In [12], the authors presented results for constant wind. In the current work, variable wind was considered. Figures 4 and 5 present examples of calculations for the case of side wind vary with height, which is described by the following formula:

$$\mathbf{w}(t) = 0.01 \cdot [0, z(t), 0]^T. \quad (72)$$

The wind profile is shown in Fig. 3.

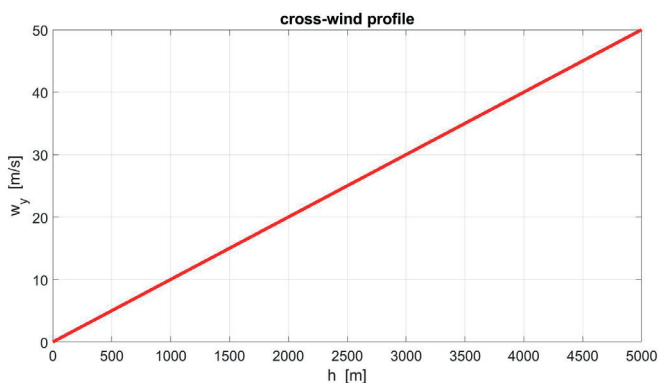


Fig. 3. The profile of the wind used in calculations

It can be seen in Fig. 4 that differences between projectile's position in consecutive time steps calculated for both, implicit and explicit, forms of the model are of the order 10^{-8} . The differences are the result of the precision¹ used in simulations. From that it can be concluded that both forms of the model give the same result.

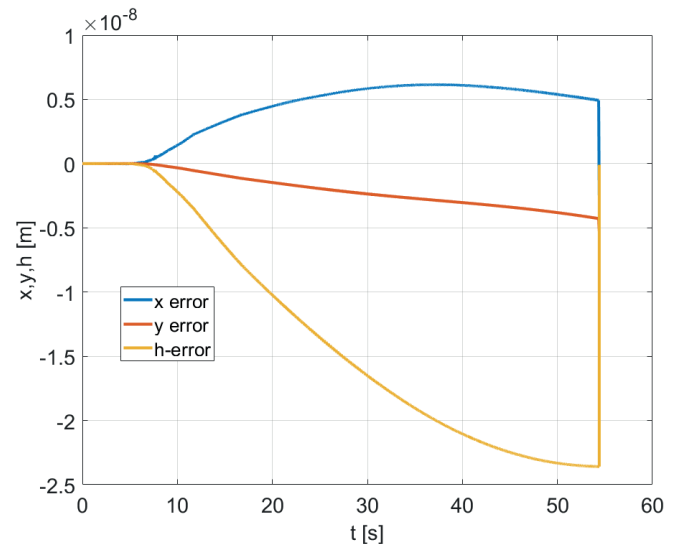


Fig. 4. Differences in projectile's position between explicit and implicit form of the model

In Fig. 5 it can be seen that utilizing explicit form of the model for inhomogeneous wind, the projectile's trajectory can be calculated up to 30% faster. This is an important feature with respect to software development for Fire Control Systems. It is important to remember that the results obtained for the calculation time are highly dependent on the hardware and algorithms

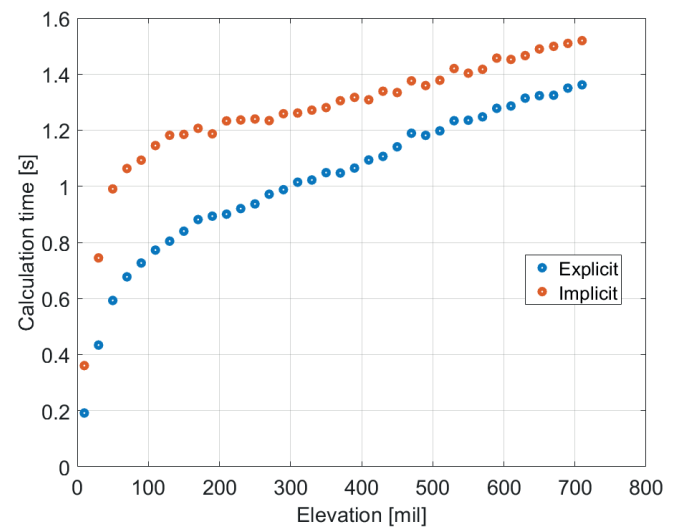


Fig. 5. Calculation time vs elevation angle

¹Tolerance set for the integration method is a measure of the error relative to the size of each solution component. Roughly, it controls the number of correct digits in all solution components.

that are used for trajectory calculation. Nevertheless, the explicit form always has significantly better performance as there is no need for applying iterative algorithms for the yaw of re- pose calculation.

Additional calculations were made to demonstrate differences in the calculation of the projectile's path in the occurrence of variable wind obtained as a result of using an incorrect mathematical model. Figures 6 and 7 present calculated projectile's trajectories in conditions of variable wind (see Eq. (72)), using the model contained in the current work and the model from [11].

Calculations were made for three different values of the elevation angle (denoted as QE): 150, 400 and 650 mils. The results of calculations according to the dependence of the article with constant wind [11] were marked with the index *m1*, while calculations according to the dependence of the current article for the variable wind were marked with the index *m2*. Of course, in the case of cross-wind, the differences in ranges are insignificant (Fig. 6), but in the lateral deviation they are large and depend on elevation angle (as can be seen in Fig. 7).

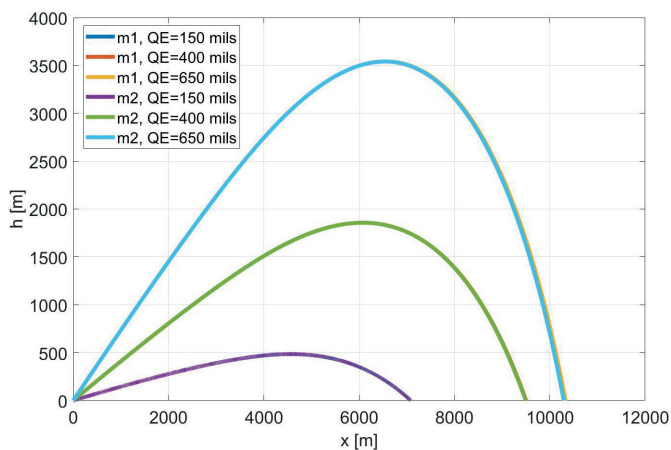


Fig. 6. Projectile flight paths taking into account variable wind for three angles of elevation (QE = 150, 400, 650 mils) – in vertical plane

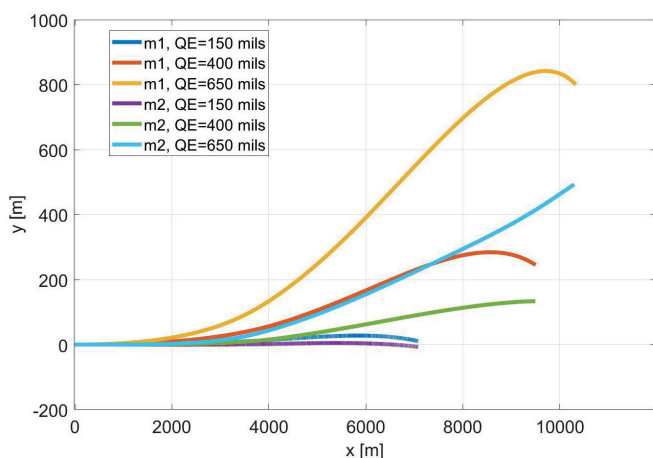


Fig. 7. Projectile flight paths taking into account variable wind for three angles of elevation (QE = 150, 400, 650 mils) – in horizontal plane

In the case of longitudinal wind, as expected, the situation is opposite, the differences in ranges were large while in the lateral deviation were insignificant.

4. Summary

This paper presented the explicit form of the modified point-mass model for the inhomogeneous wind occurring along the trajectory of the projectile. As it was pointed out in Sec. 2.3, taking into account the general wind one only needs to modify only the external forces **EF**. Therefore, the explicit form of the projectile's flight model can be easily used in the case of constant as well as inhomogeneous wind. And again, concluding the considerations contained in [11] and in this paper, the presented form of the modified point-mass model (considering the terms of aerodynamic coefficients up to $\mathcal{O}(\alpha_e^2)$ order) is much more robust and suitable for applications than its implicit form. As it was shown in Sec. 3 using the explicit form of the model can significantly decrease computational time which is a crucial factor when developing software for modern Fire Control Systems.

Acknowledgements. The paper was supported by the university research grant no. 778/2020 of Faculty of Mechatronics and Aerospace, Military University of Technology.

REFERENCES

- [1] R.L. McCoy, *Modern Exterior Ballistics. The Launch and Flight Dynamics of Symmetric Projectiles*, Schiffer Publishing, Atglen, 1999.
- [2] *STANAG 4355 – The Modified Point Mass Trajectory Model* (Ed. 3), NATO, 2002.
- [3] L. Baranowski, “Numerical testing of flight stability of spin stabilized artillery projectiles”, *J. Theor. Appl. Mech.* 51 (2), 375–385 (2013).
- [4] L. Baranowski, “Equations of motion of spin-stabilized projectile for flight stability testing”, *J. Theor. Appl. Mech.* 51 (1), 235–246 (2013).
- [5] L. Baranowski, “Effect of the mathematical model and integration step on the accuracy of the results of computation of artillery projectile flight parameters”, *Bull. Pol. Ac.: Tech.* 61 (2), 475–484, (2013).
- [6] R.F. Lieske and M.L. Reiter, “Equations of Motion for a Modified Point Mass Trajectory”, *U.S. Army Ballistic Research Laboratory*, Report No. 1314 (1966).
- [7] L. Baranowski, “Feasibility analysis of the modified point mass trajectory model for the need of ground artillery fire control systems”, *J. Theor. Appl. Mech.* 51 (3), 511–522 (2013).
- [8] H.I. Kang, G.I. Kim, and H.S. Kim, “A study on the range & deflection distance observation based on latitude position of artillery gun system”, *Int. J. Eng. Technol.* 2.12, 147–150 (2018).
- [9] M. Khalil, X. Rui, Q. Zha, H. Yu, and H. Hendy, “Projectile impact point prediction based on self-propelled artillery dynamics and Doppler radar measurements”, *Adv. Mech. Eng.* 90 (1), 203–221 (2017).
- [10] B. Konosevich and Yu. Konosevich, “Error estimate of the modified point-mass trajectory model of an artillery shell”, *Nonlinear Dyn.* 90 (1), 203–221 (2017).

Explicit form of the “modified point mass trajectory model” for the use in Fire Control Systems

- [11] L. Baranowski, B. Gadomski, P. Majewski, and J. Szymonik, “Explicit “ballistic M-model”: a refinement of the implicit “modified point mass trajectory model””, *Bull. Pol. Ac.: Tech.*, 64 (1), 81–89 (2016).
- [12] L. Baranowski, B. Gadomski, P. Majewski, and J. Szymonik, “Comparison of explicit and implicit forms of the modified point mass trajectory model”, *J. Theor. Appl. Mech.* 54 (4), 1183–1195 (2016).
- [13] L. Baranowski, B. Gadomski, P. Majewski, and J. Szymonik, “35 mm ammunition’s trajectory model identification based on firing tables”, *Bull. Pol. Ac.: Tech.* 66 (5), 635–643 (2018).
- [14] J.W. Bradley, “An alternative form of the modified point-mass equation of motion”, Ballistic Research Laboratory, Aberdeen Proving Ground, Maryland, Report No. BRL–MR–3875 (November 1990).
- [15] R.L. Pope, “The analysis of trajectory and solar aspect angle records of shell flights. Theory and computer programs”, Department of Defence, Defence Science and Technology Organisation, Weapons Systems Research Laboratory, 1978.
- [16] D. Shanks and T.S. Walton, “A new general formula for representing the drag on a missile over the entire range of Mach number”, NAVORD Report 3634, May, 1957.